

Towards Improved Text-Aligned Codebook Learning: Multi-Hierarchical Codebook-Text Alignment with Long Text

Guotao Liang^{1,2}, Baoquan Zhang^{1*}, Zhiyuan Wen², Junteng Zhao¹, Yunming Ye¹, Kola Ye³, Yao He³

¹Harbin Institute of Technology, Shenzhen ²Peng Cheng Laboratory, ³SiFar Company

lianggt@pcl.ac.cn, {baoquanzhang, yeyunming}@hit.edu.cn, 23S051042@stu.hit.edu.cn,
{wenzhiyuan2012, kolaygm, heyao18818}@gmail.com

Abstract

Image quantization is a crucial technique in image generation, aimed at learning a codebook that encodes an image into a discrete token sequence. Recent advancements have seen researchers exploring learning multi-modal codebook (i.e., text-aligned codebook) by utilizing image caption semantics, aiming to enhance codebook performance in cross-modal tasks. However, existing image-text paired datasets exhibit a notable flaw in that the text descriptions tend to be overly concise, failing to adequately describe the images and provide sufficient semantic knowledge, resulting in limited alignment of text and codebook at a fine-grained level. In this paper, we propose a novel Text-Augmented Codebook Learning framework, named TA-VQ, which generates longer text for each image using the visual-language model for improved text-aligned codebook learning. However, the long text presents two key challenges: how to encode text and how to align codebook and text. To tackle two challenges, we propose to split the long text into multiple granularities for encoding, i.e., word, phrase, and sentence, so that the long text can be fully encoded without losing any key semantic knowledge. Following this, a hierarchical encoder and novel sampling-based alignment strategy are designed to achieve fine-grained codebook-text alignment. Additionally, our method can be seamlessly integrated into existing VQ models. Extensive experiments in reconstruction and various downstream tasks demonstrate its effectiveness compared to previous state-of-the-art approaches.

1. Introduction

In recent years, vector quantization (VQ)-based image modeling has emerged as a prominent technique in the field of image generation [51]. VQ-based image modeling aims to encode continuous images into discrete code sequences using a trainable visual codebook within an encoder-

*Corresponding Authors

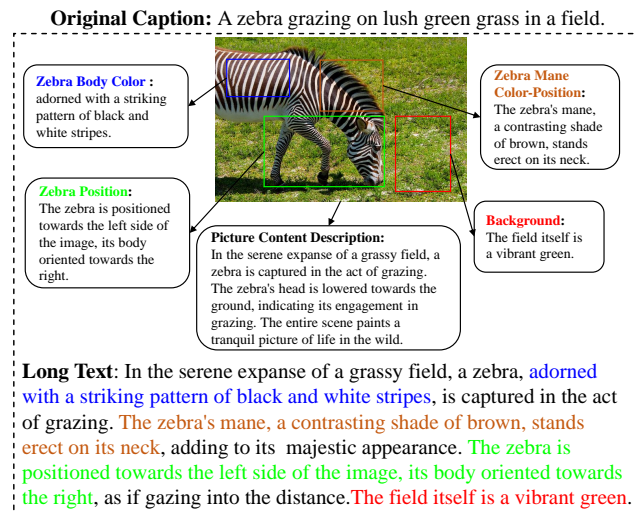


Figure 1. Example of comparing origin caption and long text. The original caption is brief and primarily provides a general description of the image. It lacks detail about the background and certain key elements within the image. In contrast, the long text can offer a more comprehensive image description, including zebra body color, position, mane color position, and background description. This additional text offers richer context, contributing to more robust and effective text-aligned codebook learning.

quantizer-decoder framework. Under this paradigm, the learned codebook, capturing rich image features, can be leveraged to generate high-fidelity images through auto-regression [12, 13, 47] or discrete diffusion methods[17].

To further enhance the performance of VQ-based methods, several innovative techniques and ideas [18, 31, 34] have been introduced to learn a more robust codebook representation, such as introducing adversarial loss [13], learning compact code sequence [22, 23], or dealing with codebook collapse [24, 49, 60, 63, 65]. Different from the aforementioned methods that only learn single-modal codebook, Liang *et al.* [29] propose LG-VQ, which incorporates pre-trained text semantics to learn text-aligned codebook, thereby improving the performance of VQ-based models in

various cross-modal downstream tasks.

Despite the success of LG-VQ, it has limitations regarding insufficient alignment between codebook and text, primarily due to the brevity of the existing image captions. As illustrated in Fig. 1, we can see that the original caption is concise, focusing solely on the main object while omitting details about the background and other key elements of the image. This brevity results in a lack of sufficient semantic information, hindering the learning of a well text-aligned codebook. Inspired by recent visual-language models (VLMs) [5, 16, 68], we propose utilizing VLMs to generate more detailed description for each image, as depicted in Fig. 1. Compared to the original caption, the augmented text provides a more comprehensive description of the image. Resorting to such longer text, richer semantic knowledge can be obtained to learn more robust codebook representation and achieve improved text-aligned codebook.

However, the augmented text usually contains hundreds of words, making it challenging for pre-trained language models [9, 43] to capture and retain all key semantic information during encoding. Additionally, encoding and using such lengthy text imposes a significant computational burden. To address this issue, we propose splitting the long text into multiple granularities for encoding, *i.e.*, word, phrase, and sentence. Its advantage is that the long text semantics can be fully encoded without losing any key semantic knowledge by resorting to different granularities. Unfortunately, we are in another dilemma. The multi-granularity text semantics and single code sequence semantics are structurally inconsistent, making direct alignment more difficult. To handle this, we propose a hierarchical encoder that encodes images into multi-hierarchical code representations, each hierarchy corresponding to a specific semantic granularity text. This design ensures a more precise and structurally consistent alignment relationship between image codes and multi-granularity text semantics. Based on the consistent alignment relationship, we propose a novel sampling-based alignment strategy, which can achieve fine-grained codebook-text alignment while not introducing much computational overhead. As a result, a novel text-augmented codebook learning framework, termed *Text-Augmented VQ (TA-VQ)*, is proposed for improved text-aligned codebook learning.

In a nutshell, we summarize our main contributions as:

- We propose a novel text-augmented codebook learning framework, TA-VQ, which leverages VLMs to generate longer text for each image, improving text-aligned codebook learning. This approach enables 1) fine-grained alignment through detailed image descriptions, and 2) richer semantic knowledge for robust codebook learning.
- We propose to encode long text semantics at three granularities, *i.e.*, word, phrase, and sentence, aiming to retain all key semantic knowledge. Resorting to this multi-

granularity text semantics, a hierarchical encoder and novel sampling-based alignment strategy are designed to achieve fine-grained codebook-text alignment.

- We conduct comprehensive experiments on three public datasets, demonstrating that our method surpasses previous state-of-the-art models in reconstruction quality and performance across various downstream tasks.

2. Related Works

2.1. Vector Quantization for Image Generation

Vector quantization (VQ) plays a crucial role in image generation by compressing continuous images into discrete token sequences using a learnable codebook [3, 17, 27, 57]. Oord *et al.* [51] introduced VQ-VAE, an encoder-quantizer-decoder architecture for vector quantization. However, VQ-VAE is limited in generating high-fidelity images due to the insufficient codebook representation. Subsequently, various methods [13, 19, 22, 23, 29, 31] have been proposed to enhance image generation quality. For instance, Esser *et al.* [13] propose VQ-GAN, integrating adversarial and perceptual losses based on VQ-VAE, which significantly improves the quality of image generation. CVQ [65] addresses codebook collapse by selecting encoded features as anchors to update “dead” code representations. VQCT [60] introduces pre-trained word semantics as the initial codebook and then utilizes the semantic relationship of words to achieve cooperative optimization between codes to eliminate the codebook collapse issue. Recently, some researchers [32, 58, 69] explore mapping the images to the word tokens of LLMs by viewing images as “foreign languages” to improve the performance of the codebook on downstream tasks with the help large language models (LLMs). Unlike the aforementioned methods that focus solely on single-modal codebook learning, Liang *et al.* [29] propose a novel multi-modal codebook learning framework, called LG-VQ, by introducing pre-trained text semantics as supervised information, which significantly improves the performance of VQ-based models in various cross-modal downstream tasks.

In this paper, we also focus on learning text-aligned codebook. Different from the existing methods that rely on limited image captions, our approach leverages the VLMs to extend the text description for each image and proposes a novel alignment method to efficiently encode and exploit the semantics of extended texts for improving text-aligned codebook learning.

2.2. Visual-Language Models

Inspired by the success of Large Language Models (LLMs) in the field of natural language processing [2, 11, 45, 50], lots of researchers [5, 16, 68] have begun to explore integrating visual information into LLMs to form Visual Language Models (VLMs) for jointly solving various multi-

modal tasks, such as visual grounding [8], visual question answering [37], image description [39], etc. There are currently two fusion strategies, *i.e.*, token-level and feature-level fusion. The token-level refers to the visual features being transformed into tokens, which LLMs can understand, through a learnable Adapter Network, and then are concatenated with text tokens and fed into LLMs. This learnable Adapter Network includes Q-Former [4, 7, 28, 62] and MLP [33, 41, 48, 64]. The feature-level refers to inserting extra modules to enable text and visual features to interact more deeply, such as cross-attention layers [1], visual expert module [54]. These VLMs have shown powerful capabilities in handling various visual understanding tasks.

In this paper, we propose to employ VLMs to generate more detailed descriptions for each image. The advantage is that longer text can bring richer semantic knowledge for more robust codebook learning.

3. Preliminaries

3.1. VQ-VAE

VQ-VAE [51] trains a visual codebook to encode the image into a discrete code sequence through an encoder-quantizer-decoder framework. As illustrated in Fig. 2, the codebook is defined as $C = \{(k, e_k)\}_k^K$ which consists of learnable K entries $e_k \in \mathbb{R}^{d_z}$ with dimension d_z . Given an input image $x \in \mathbb{R}^{H \times W \times C}$, where H , W , and C represent the height, width, and channel of the image respectively. The encoder $E_{\theta_e}(\cdot)$ with parameter θ_e and down-sampling factor f , which gradually compress the original image into a grid feature $\hat{Z} = E_{\theta_e}(x) \in \mathbb{R}^{\frac{H}{f} \times \frac{W}{f} \times d_z}$. The quantizer $Q(\cdot)$ replaces each grid feature with a code representation based on the distance between \hat{Z} and C . That is:

$$z_i = Q(\hat{z}_i) = \underset{e_k \in C}{\operatorname{argmin}} \|\hat{z}_i - e_k\|. \quad (1)$$

As a result, quantized code representation Z can be obtained, the decoder $D_{\theta_d}(\cdot)$ with parameter θ_d is employed to reconstruct the input image by $\tilde{x} = D_{\theta_d}(Z)$. The whole network is optimized by minimizing the following objective:

$$\mathcal{L}_{vq} = \|x - \tilde{x}\|_2^2 + \|sg[E_{\theta_e}(x)] - Z\|_2^2 + \beta \|E_{\theta_e}(x) - sg[Z]\|_2^2, \quad (2)$$

where β is a hyper-parameter, $sg[\cdot]$ denotes the stop-gradient operator. The first term is reconstruction loss, the second is codebook loss, which encourages the codebook to be close grid features, and the third is the ‘‘commitment loss’’ [51]. Recently, some researchers introduce pre-trained text semantics to learn text-aligned codebook. However, such concise text fails to provide sufficient semantic knowledge, resulting in insufficient codebook-text alignment.

3.2. Wasserstein distance

The Wasserstein distance [15, 56], known as Earth Mover’s Distance (EMD), measures the distance between two probability distributions or sets of weighted objects. The computation of the Wasserstein distance relies on solving the well-known transportation problem [21]. Specifically, suppose we have a set of suppliers $H = \{h_1, h_2, \dots, h_n\}$, where h_i denotes supply good capacity of the i -th supplier. These suppliers need to provide goods to multiple consumers, and the quantity of goods required by each consumer is fixed $Q = \{q_1, q_2, \dots, q_m\}$, where q_j indicates the amount needed by the j -th consumer. The cost of transporting one good unit from supplier i to consumer j is represented by γ_{ij} . The transportation problem is to find a least-expensive flow of goods $F = \{f_{ij} | i = 1, \dots, n, j = 1, \dots, m\}$ from the suppliers to the consumers that satisfy the consumers’ demand:

$$\begin{aligned} & \underset{f_{ij}}{\operatorname{minimize}} && \sum_{i=1}^n \sum_{j=1}^m \gamma_{ij} f_{ij} \\ & \text{subject to} && f_{ij} \geq 0, i = 1, \dots, n, j = 1, \dots, m \\ & && \sum_{j=1}^m f_{ij} = h_i, \quad i = 1, \dots, n \\ & && \sum_{i=1}^n f_{ij} = q_j, \quad j = 1, \dots, m. \end{aligned} \quad (3)$$

We can solve the Linear Programming problem or use some approximate algorithms [6, 14, 25] to obtain the optimal flow of goods F . In our paper, we adopt Wasserstein distance to achieve the alignment between codebook and text.

4. Proposed Method: TA-VQ

Existing works attempt to improve codebook performance in downstream tasks by learning text-aligned codebook. However, these methods overlook the limitation of overly concise text descriptions (see Fig. 1 for more details), which provide insufficient semantic information for codebook-text alignment. To address this, we propose TA-VQ, a novel codebook learning framework that generates longer text to improve codebook-text alignment. As illustrated in Fig. 2, our TA-VQ consists of three key steps, *i.e.*, text generation, multi-granularity text encoding, and semantic alignment. Here, we elaborate on each step in order:

Step 1: Text Generation. Different from existing works that adopt limiting text semantics, we employ ShareGPT4V [5] to generate longer and more detailed text for each image, improving text-codebook alignment. Specifically, following the ShareGPT4V, we construct a generic prompt that describes the image: ‘‘Analyze the image in a comprehensive and detailed manner’’. Then we feed the image and constructed prompt into ShareGPT4V to generate extended text descriptions. Notably, the same prompt is uniformly applied to all images.

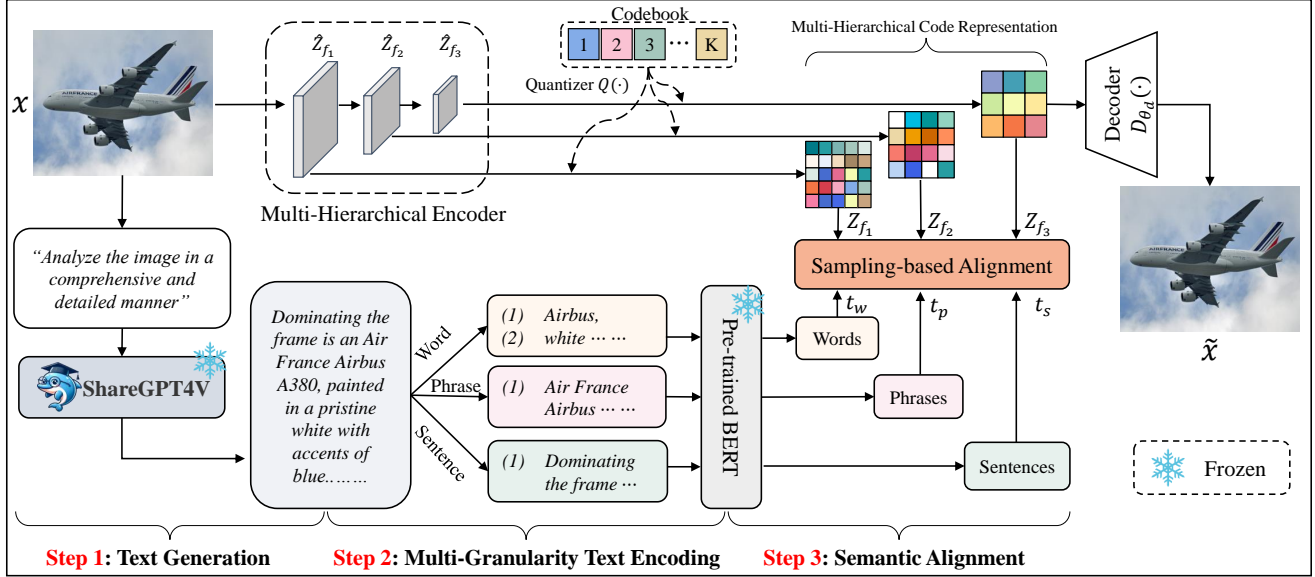


Figure 2. The illustration of our proposed TA-VQ framework. The image is first fed to VLM to generate a more detailed text description, and then the text is split into multiple granularities for encoding, *i.e.*, word (t_w), phrase (t_p), and sentence semantics (t_s). Subsequently, the multi-hierarchical encoder encodes and quantizes the image into multi-hierarchical code representation, *i.e.*, Z_{f_1} , Z_{f_2} , and Z_{f_3} . The sampling-base alignment module is employed to achieve Z_{f_1} , Z_{f_2} , Z_{f_3} and t_w , t_p , t_s alignment. Finally, the decoder is used to reconstruct the origin image using Z_{f_3} .

Step 2: Multi-Granularity Text Encoding. Although the generated long text can provide richer semantic knowledge, it also brings a key challenge, that is, how to effectively encode the text. To address this, we propose to split the long text into multiple granularities for encoding, *i.e.* word, phrase, and sentence. Specifically, given a long text t , we employ a text process tool (*i.e.*, TextBlob [36]) to extract all sentences and phrases. Following this, the BERT language model [9] is employed to encode them. As a result, the sentence and phrase semantics can be obtained, which is denoted by $t_s = \{s_1, s_2, \dots, s_{|t_s|}\}$, where $s_i \in \mathbb{R}^d$ denotes i -th sentence representation with dimension d , and $t_p = \{p_1, p_2, \dots, p_{|t_p|}\}$, where $p_i \in \mathbb{R}^d$ denotes i -th phrase representation, respectively. For word granularity, inspired by [60], we focus on extracting visual-relevant words, such as nouns, adjectives, and quantifiers, rather than encoding all words. As a result, the word semantic can be obtained by BERT pre-trained word embedding, which is denoted by $t_w = \{w_1, w_2, \dots, w_{|t_w|}\}$, where $w_i \in \mathbb{R}^d$ denotes i -th word representation. Resorting to text semantics of different granularities, the long text can be effectively encoded without losing any key semantic knowledge, which is beneficial for achieving fine-grained alignment.

Step 3: Semantic Alignment. As previously discussed, structurally inconsistent alignment relationships exist between single code sequence semantics and multi-granularity text semantics, making it difficult to align directly. To solve this, as shown in Fig. 2, we propose a hierarchical encoder

that encodes and quantizes images into multi-hierarchical code representation, where each hierarchy corresponds to a specific granularity text semantic. This design leverages the inherent hierarchical structure of image encoding, where lower layers model basic semantics and deeper layers encode more abstract semantic features. This hierarchical structure mirrors the semantic hierarchical structure from word to phrase to sentence in the natural language. The key advantage of this design is that it enables a more precise and structurally consistent alignment relationship between image codes and multi-granularity text semantics. Formally, given an image, we first encode it into three hierarchical grid features, denoted as $\hat{Z}_h = \{\hat{Z}_{f_1}, \hat{Z}_{f_2}, \hat{Z}_{f_3}\}$, where $\hat{Z}_{f_j} \in \mathbb{R}^{\frac{H}{f_j} \times \frac{W}{f_j} \times d_z}$ and $f_j \in \{4, 8, 16\}$. Here, the \hat{Z}_{f_1} captures the feature from the lower layers, while \hat{Z}_{f_3} represents the feature from deeper layers. As a result, the multi-hierarchical image code representation can be obtained by Eq. (1), which is denoted by $Z_h = \{Z_{f_1}, Z_{f_2}, Z_{f_3}\}$. Each hierarchical image code is then aligned with the corresponding granularity of text semantics (*i.e.*, words, phrases, and sentences) based on a sampling-based alignment strategy. The details of the sampling-based alignment strategy will be elaborated in Sec. 4.1.

4.1. Sampling-based Alignment Strategy

In this subsection, we introduce how to align multi-hierarchical image code representation (*i.e.*, Z_{f_1} , Z_{f_2} , Z_{f_3}) and multi-granularity text semantics (*i.e.*, t_w , t_p , t_s). Since

the alignment process is consistent across different granularities, we use the alignment between the Z_{f_3} and sentences t_s as an illustration.

Actually, Z_{f_3} and t_s have unequal numbers (*i.e.*, $|Z_{f_3}| \neq |t_s|$), and there is no explicit alignment relationship in the dataset, making it impossible to measure the distance between them for optimization directly. One straightforward approach might involve computing the distance based on the mean representation of them, but this method overlooks critical local semantic information. To solve this problem, we formulate the semantic alignment problem as an optimal transport problem [52], *i.e.*, minimizing the transport cost from codebook representation to text representation to achieve codebook-text semantic alignment. Following this idea, the Wasserstein distance is employed to calculate the optimal transport cost between Z_{f_3} and t_s . According to the description in Sec. 3.2, we can regard Z_{f_3} as the suppliers, t_s as the consumers, and the cost of transporting one good unit is measured by the pairwise distance between the i -th code representation and j -th sentence representation $\gamma_{ij} = \|z_i - s_j\|_2$. Following [61], we can embed the solution process of optimal flow F into the neural network so that the transport cost can be minimized to achieve semantic alignment of codebook and text.

Complexity Problem. As mentioned above, considering the worst case, solving such an optimal flow F has a complexity of $O(\max(|Z_{f_3}|^3, |t_s|^3))$. It is important to note that the computational burden arises primarily from the term $|Z_{f_3}|$. To address this challenge, we draw inspiration from the work of Lu & Lu [38], which demonstrates that there exists a specialized feedforward neural network (FNN) so that the Wasserstein distance between a continuous distribution μ and a discrete distribution ν is small enough, as formally stated in Theorem 1. We regard t_s as a discrete distribution and propose modeling Z_{f_3} as a Gaussian Distribution, from which we can sample $|t_s|$ feature vectors using the reparameterization trick [26]. Then, we can use the sampled feature vectors to calculate the Wasserstein distance. Its advantage is that the computational complexity is reduced from $O(|Z_{f_3}|^3)$ to $O(|t_s|^3)$. To further reduce the computational burden, we propose to sample q samples from t_s instead of using the entire t_s . So that the computational burden is further reduced to $O(q^3)$. Specifically, as shown in Fig. 3, we equip FNNs to model Z_{f_3} as a Gaussian Distribution:

$$\begin{aligned} m_{f_3} &= \text{Mean}(Z_{f_3}), \\ \mu_{f_3} &= \text{FNN}_\mu^{f_3}(m_{f_3}), \\ \Sigma_{f_3} &= \text{diag}(\exp(\text{FNN}_\sigma^{f_3}(m_{f_3}))). \end{aligned} \quad (4)$$

Then, according to the Theorem 1, we define the sentence information t_s as a discrete distribution, denoted by $\mathcal{P}_{t_s} \triangleq \frac{1}{|t_s|} \sum_{s \in t_s} \delta_s$. Based on the above sampling idea, we sample q target sentence semantics from \mathcal{P}_{t_s} instead

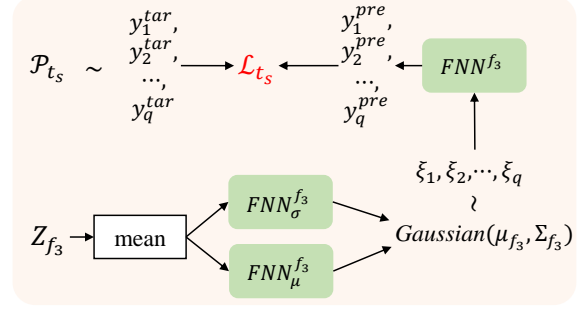


Figure 3. Illustration of the Sampling-based Alignment Strategy.

of using the entire set, denoted as $\{y_i^{tar} | 1 \leq i \leq q\}$. Next, we also obtain q samples from Gaussian Distribution $\mathcal{N}(\mu_{f_3}, \Sigma_{f_3})$ using reparameterization trick [26], denoted as $\{\xi_i \sim \mathcal{N}(\mu_{f_3}, \Sigma_{f_3}) | 1 \leq i \leq q\}$. Following [56], we feed each ξ_i into FNN to get q prediction information, denoted as $\{y_i^{pre} = \text{FNN}^{f_3}(\xi_i) | 1 \leq i \leq q\}$. To this end, we can minimize the Wasserstein distance between y^{tar} and y^{pre} to achieve semantic alignment of Z_{f_3} and t_s . That is:

$$\mathcal{L}_{t_s} = \mathcal{W}(y^{pre}, y^{tar}). \quad (5)$$

Finally, we apply the Sinkhorn-Knopp algorithm [6] to approximate the solution, whose complexities are $O(q^2)$.

Theorem 1 *Let $\mu \in \mathcal{P}_2(\mathbb{R}^d)$ be absolutely continuous with respect to the Lebesgue measure with Radon–Nikodym density $\rho(x)$. Let $\nu = \sum_{i=1}^n \nu_i \delta_{y_i}$ for some $\{y_j\}_{j=1}^n \subset \mathbb{R}^d$, $\nu_j \geq 0$ and $\sum_{j=1}^n \nu_j = 1$, where δ is Dirac delta function. Then, for any $\epsilon > 0$, there exists a fully connected deep neural network $u(\cdot) : \mathbb{R}^d \rightarrow \mathbb{R}$ with sufficiently large width and depth (depending on $\epsilon > 0$) such that the Wasserstein distance between $\nabla u(\mu)$ and ν is less than ϵ , where $\nabla u(\cdot)$ is gradient of $u(\cdot)$.*

4.2. Training Objective

Following the above process, we can also calculate the loss \mathcal{L}_{t_w} (*i.e.*, Z_{f_1} and words t_w) and \mathcal{L}_{t_p} (*i.e.*, Z_{f_2} and phrases t_p). We use three hyperparameters (*i.e.*, α , β , and γ) to control three semantic alignment losses, respectively. Finally, the overall objective function is:

$$\mathcal{L} = \mathcal{L}_{vq} + \alpha \mathcal{L}_{t_w} + \beta \mathcal{L}_{t_p} + \gamma \mathcal{L}_{t_s}. \quad (6)$$

5. Experiments

5.1. Experimental Settings

Benchmarks. Our method is model-agnostic, allowing it to be applied to different VQ-based architectures. Then, we choose VQ-GAN [13] and CVQ [65] as our backbone networks. Additionally, our method incorporates pre-trained text semantics, to ensure a fair comparison, we use recent works LG-VQ [29]_{NeurIPS'2024} and VQCT [60]_{CVPR'2024}

as baselines, both of which also leverage language materials and the pre-trained language model. We evaluate our method on three public datasets for image reconstruction, including CelebA-HQ [35], CUB-200 [53], and MS-COCO [30]. We also evaluate our method on various downstream tasks based on the learned codebook, including text-to-image, semantic synthesis, unconditional image generation, and image completion on CelebA-HQ [35], and image captioning on CUB-200 [53], and visual grounding on refcoco dataset [59], and visual question answering (VQA) on COCO-QA dataset [46].

Evaluation Metrics. Following previous works [13, 60, 63, 65], we adopt the standard Fréchet Inception Distance (FID) [20] to evaluate the quality of image reconstruction and generation. For other downstream tasks, such as visual grounding, image captioning, and VQA, we follow the evaluation strategy outlined in [29].

Implementation Details. Following VQ-GAN and LG-VQ [13, 29], all images are reshaped 256×256 for reconstruction and generation. We set the down-sampling factor f to 16 and the codebook size K to 1024, with a batch size of 6. The architecture of TA-VQ exactly follows VQ-GAN except for the proposed hierarchical encoder and semantic alignment module. All FNNs are 2-layer multilayer perceptron (MLP) with ReLU activation function. The three key hyperparameters (α , β , and γ) are uniformly set to 0.001 across all datasets. For further details regarding the generated text, please refer to the supplementary materials.

5.2. Discussion of Results

Table 1 compares our method and the state-of-the-art VQ-based method in image reconstruction performance. From the results, we can obtain several key conclusions: 1) Compared with the backbone network (*i.e.*, VQ-GAN, and CVQ), our method can learn more robust codebook representation by introducing pre-trained text semantics to significantly improve reconstruction performance, indicating the effectiveness of our method; 2) Our method surpasses LG-VQ across all datasets, largely due to its ability to integrate long text with richer semantic knowledge and effectively encode them at different granularities to learn more robust codebook learning; 3) Compared to VQCT, our method can achieve lower reconstruction errors when using the CVQ backbone, which suggests the effectiveness and generality of method. Notably, our method achieves superior reconstruction and significantly enhances codebook performance across various downstream tasks, suggesting our method’s effectiveness. Further qualitative comparisons are provided in the supplementary materials.

5.3. Ablation Study

Are our semantic alignments of words, phrases, and sentences both effective? We conduct extensive ablation stud-

Models	Codebook		CelebA-HQ	CUB-200	MS-COCO
	Size	#Tokens	FID↓	FID↓	FID↓
VQCT [60]	6207	512	5.02	4.52	9.82
VQ-GAN [13]	1024	256	5.66	5.31	14.45
LG-VQ [29]	1024	256	5.34	4.74	10.72
TA-VQ (Ours)	1024	256	5.03	4.60	10.32
CVQ [65]	1024	256	5.19	4.64	9.94
LG-CVQ [29]	1024	256	4.90	4.40	9.69
TA-CVQ (Ours)	1024	256	4.71	4.03	9.65

Table 1. Results (FID↓) of image reconstruction on CelebA-HQ, CUB-200, and MS-COCO. The best results are highlighted in bold.

Setting		CUB-200
		FID↓
(i)	Baseline(VQ-GAN)	5.51
(ii)	+ \mathcal{L}_s	4.89
(iii)	+ $\mathcal{L}_s + \mathcal{L}_p$	4.69
(iv)	+ $\mathcal{L}_s + \mathcal{L}_w$	4.82
(v)	+ $\mathcal{L}_w + \mathcal{L}_p$	4.75
(vi)	+ $\mathcal{L}_w + \mathcal{L}_p + \mathcal{L}_s$	4.60

Table 2. Ablation study of our three loss functions on CUB-200. “+ \mathcal{L}_s ” denotes introduces the sentence semantic alignment into the baseline model.

ies to evaluate the impact of three semantic losses, as summarized in Tab. 2. We use VQ-GAN as the baseline model, without incorporating any additional semantic losses. From the results, several key conclusions can be drawn: First, all three semantic losses are essential for enhancing reconstruction performance. Second, the results of (i) to (iv) show that sentence-level semantics (\mathcal{L}_s) contribute the most to performance improvement. This can be attributed to the richer, high-level semantic information sentences provide, which supports more robust codebook learning. Furthermore, because the alignment takes place at the level of codes (Z_{f_3}) used for reconstruction, the semantic knowledge can directly be utilized to improve reconstruction quality. Finally, comparing (vi) with (i) to (v), we observe that incorporating all three losses results in the best overall performance, demonstrating the effectiveness of our method.

Is our multi-granularity text encoding method effective?

To answer the question, we analyze the impact of not having multi-granularity text encoding, *i.e.* using the entire long text semantics directly aligned with the image codes. The results are shown in Tab. 3, we can observe that considering multi-granularity text encoding can achieve better reconstruction, which is reasonable because such encoding manner can effectively retain all key semantic knowledge. This shows the effectiveness of our method.

Can our codebook be effectively aligned with the text?

In Tab. 4, we measure the cosine similarity between the codebook and text on CUB-200 all test data. From the results, we can see that TA-VQ’s codebook is more similar to the text than LG-VQ, indicating that our method can learn

Setting	FID↓
w/o multi-granularity	4.91
TA-VQ	4.60

Table 3. Ablation study of multi-granularity text encoding on CUB-200. “w/o” means without.

Setting	Similarity↑
LG-VQ [29]	0.1021
TA-VQ	0.1444

Table 4. Ablation study of cosine similarity evaluation between codebook and text on CUB-200.

Setting	#Train time sec/epoch↓
w/o sampling	2,065
TA-VQ	1,930

Table 5. Ablation study of computational overhead without and with sampling strategy.

Model	Image Completion
	FID↓
VQ-GAN	9.02
LG-VQ	8.14
TA-VQ	8.04

Table 6. Result (FID↓) of image completion on CelebA-HQ.



Figure 4. Examples of unconditional generation on CelebA-HQ. More examples are provided in supplementary materials.



Figure 5. Examples of semantic synthesis (row 1), text-to-image (row 2), and image completion (row 3). More examples are provided in supplementary materials.

better text-aligned codebook.

Can our sampling-based alignment strategy reduce the computational overhead? To answer the question, we conduct an experiment without and with sampling alignment strategy with a batch size equal to 1 on the CUB-200 dataset. The experiments are conducted on Debian GNU/Linux 12 with Intel(R) Core(TM) i9-10900X CPU, a GTX 4090, and 128G memory. We calculate the seconds required for both methods to train one epoch, the results are shown in Tab. 5, which suggests our design of sampling-based alignment strategy can effectively reduce the computational overhead.

5.4. Application

To further assess the effectiveness of our method, we apply the codebook learned by our method to various downstream tasks, including image generation, visual grounding, and visual text reasoning. We select the VQ-GAN as the backbone network, named TA-VQ.

5.4.1 Image Generation

Following [13, 17, 29, 47], we conduct image generation downstream tasks, *i.e.* image completion, unconditional and conditional image generation, to verify the effectiveness of

our method.

Image Completion and Unconditional Generation . We follow the default setting of VQ-GAN-transformer [13] and conduct image completion and unconditional image generation on CelebA-HQ. The results are shown in Tab. 6 and Tab. 7, respectively. From the results, our method can achieve superior performance, which indicates that our approach can more effectively leverage text semantics to learn a robust codebook representation, suggesting the effectiveness of our method. In comparison to LG-VQ, our method can further improve performance, which confirms our motivation for using longer text. Examples of Unconditional generation are shown in Fig. 4. We also provide a qualitative comparison of image completion in Fig. 5 row 3. **Conditional Generation.** We further evaluate the performance of our codebook on two tasks: semantic synthesis [13] and text-to-image generation [17]. For the semantic synthesis task, we follow the default settings of VQ-GAN-transformer, with results provided in Tab. 8. TA-VQ achieves the best performance compared to other models. This can be attributed to our multi-granularity encoding design, which fully leverages the rich semantic information in long texts for more robust codebook learning. For the text-to-image task, we use VQ-diffusion [17] as the backbone network, with results shown in Tab. 10. TA-VQ achieves a lower FID score, primarily due to our multi-hierarchical semantic alignment module, which enables a more comprehensive understanding of text conditions. This supports the effectiveness of our method. Qualitative comparison of conditional generation can be found in Fig. 5 row 1 and row 2.

5.4.2 Visual Grounding

We conduct a visual grounding task on refcoco dataset [59] utilizing MS-COCO’s codebook. The evaluation metric follows prior work [8, 29], where a prediction is considered correct if the IoU between the ground truth box and the predicted bounding box exceeds 0.5. We select VQ-GAN, VQCT, and LG-VQ as baseline. The results are shown in Tab. 9, TA-VQ achieves the best performance compared with baseline models. We provide a qualitative comparison in Fig. 6, which shows TA-VQ achieves more accurate predictions. This confirms the advantage of introducing longer text to learn an improved text-aligned codebook.

Model	Unconditional Generation
	FID↓
DC-VAE [42]	15.8
VQ-GAN [13]	10.2
LG-VQ [29]	9.1
TA-VQ	8.8

Table 7. Result (FID↓) of unconditional image generation on CelebA-HQ.

Model	Semantic Synthesis
	FID↓
VQCT [60]	14.47
VQ-GAN [13]	11.53
LG-VQ [29]	11.46
TA-VQ	10.74

Table 8. Result (FID↓) of semantic synthesis on CelebA-HQ.

Model	Visual Grounding
	Accuracy(0.5)↑
VQ-GAN [13]	9.14
VQCT [60]	9.46
LG-VQ [29]	9.62
TA-VQ	10.17

Table 9. Result of visual grounding on refcoco dataset [59].

Model	Text-to-Image
	FID↓
Corgi [67]	19.74
LAFITE [66]	12.54
VQ-GAN [13]	15.29
CVQ [65]	13.23
LG-VQ [29]	12.61
TA-VQ	11.97

Table 10. Results (FID↓) of text-to-image on CelebA-HQ.

Model	Image Captioning			
	BLEU4↑	ROUGE-L↑	METEOR↑	CIDEr-D↑
VQ-GAN [13]	1.29	33.40	24.47	93.62
VQCT [60]	1.38	26.50	24.63	98.22
LG-VQ [29]	1.69	34.73	25.78	102.77
TA-VQ	1.90	35.50	27.61	109.42

Table 11. Results of image captioning on CUB-200 datasets.

Setting	VQA	
	Accuracy↑	WUPS↑[55]
VQCT [60]	40.42	82.06
VQ-GAN [13]	37.82	83.22
LG-VQ [29]	40.97	83.56
TA-VQ	41.56	83.77

Table 12. Results of VQA on COCO-QA [46] dataset.

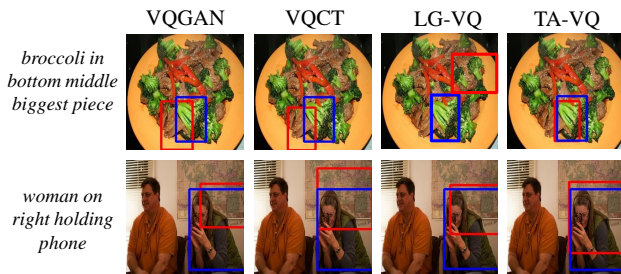


Figure 6. Visualizations for visual grounding. The blue boxes are the ground-truth, red boxes are the model predictions. More Examples are provided in supplementary materials.

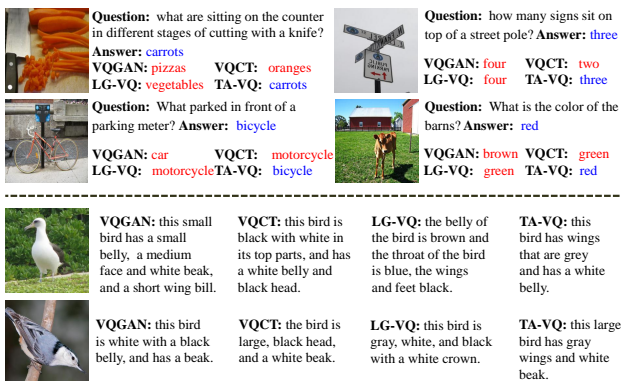


Figure 7. Visualizations for VQA, and image captioning. More Examples are provided in supplementary materials.

5.4.3 Visual Text Reasoning

To fully verify the effectiveness of the learned codebook, following [10, 29, 39], we conduct two visual text reason-

ing tasks, *i.e.*, image captioning on CUB-200, and visual question answering (VQA) on COCO-QA dataset [46] using MS-COCO’s codebook. Following [29], we use a pre-trained language model (*e.g.*, GPT2 [44]) as the backbone network. We select VQ-GAN, VQCT, and LG-VQ as baseline. The results are shown in Tab. 11 for image captioning and Tab. 12 for VQA. From the results, we can see that our method outperforms the baseline models on all tasks. This is likely because the design of multi-granularity text encoding and sampling-based alignment enhances the model’s ability to achieve fine-grained codebook-text alignment, which improves the performance of cross-modal tasks. Finally, we provide some examples in Fig. 7, which shows that our method can accurately generate text with consistent semantics with the image in the image captioning, and can accurately answer the question in the VQA. This confirms the effectiveness of our approach.

6. Conclusions

This paper proposes a novel text-augmented codebook learning framework, named TA-VQ, which utilizes VLMs to generate longer text for improved text-aligned codebook learning. In particular, we propose to encode the long text semantics from three granularities, *i.e.*, word, phrase, and sentence. Moreover, we also design a novel sampling-based alignment strategy for achieving fine-grained codebook text alignment, which does not introduce much computational overhead. Both quantitative and qualitative experiments show that our approach achieves superior reconstruction and substantially improves codebook performance across various downstream tasks, demonstrating the effectiveness of our method.

References

- [1] Jean-Baptiste Alayrac, Jeff Donahue, Pauline Luc, Antoine Miech, Iain Barr, Yana Hasson, Karel Lenc, Arthur Mensch, Katherine Millican, Malcolm Reynolds, et al. Flamingo: a visual language model for few-shot learning. *Advances in neural information processing systems*, 35:23716–23736, 2022. 3
- [2] Tom B Brown. Language models are few-shot learners. *arXiv preprint arXiv:2005.14165*, 2020. 2
- [3] Huiwen Chang and Han Zhang. Maskgit: Masked generative image transformer. In *CVPR*, pages 11315–11325, 2022. 2
- [4] Feilong Chen, Minglun Han, Haozhi Zhao, and Qingyang Zhang. X-llm: Bootstrapping advanced large language models by treating multi-modalities as foreign languages. *arXiv preprint arXiv:2305.04160*, 2023. 3
- [5] Lin Chen, Jisong Li, Xiaoyi Dong, Pan Zhang, et al. Sharegpt4v: Improving large multi-modal models with better captions. *arXiv preprint arXiv:2311.12793*, 2023. 2, 3
- [6] M Cuturi. Lightspeed computation of optimal transportation distances. *Advances in Neural Information Processing Systems*, 26(2):2292–2300, 2013. 3, 5
- [7] Wenliang Dai and Junnan Li. Instructblip: Towards general-purpose vision-language models with instruction tuning. *CoRR*, abs/2305.06500, 2023. 3
- [8] Jiajun Deng, Zhengyuan Yang, Tianlang Chen, Wengang Zhou, and Houqiang Li. Transvg: End-to-end visual grounding with transformers. In *CVPR*, pages 1769–1779, 2021. 3, 7
- [9] Jacob Devlin and Ming-Wei Chang. Bert: Pre-training of deep bidirectional transformers for language understanding. *arXiv preprint arXiv:1810.04805*, 2018. 2, 4
- [10] Ming Ding and Zhuoyi Yang. Cogview: Mastering text-to-image generation via transformers. *NeurIPS*, 34:19822–19835, 2021. 8
- [11] Abhimanyu Dubey, Abhinav Jauhri, Abhinav Pandey, Abhishek Kadian, Ahmad Al-Dahle, Aiesha Letman, Akhil Mathur, Alan Schelten, Amy Yang, Angela Fan, et al. The llama 3 herd of models. *arXiv preprint arXiv:2407.21783*, 2024. 2
- [12] Omar Elharrouss and Noor Almaadeed. Image inpainting: A review. *Neural Processing Letters*, 51:2007–2028, 2020. 1
- [13] Patrick Esser, Robin Rombach, and Bjorn Ommer. Taming transformers for high-resolution image synthesis. In *CVPR*, pages 12873–12883, 2021. 1, 2, 5, 6, 7, 8
- [14] Haoqiang Fan, Hao Su, and Leonidas J Guibas. A point set generation network for 3d object reconstruction from a single image. In *CVPR*, pages 605–613, 2017. 3
- [15] Charlie Frogner, Chiyuan Zhang, Hossein Mobahi, Mauricio Araya, and Tomaso A Poggio. Learning with a wasserstein loss. *Advances in neural information processing systems*, 28, 2015. 3
- [16] Rohit Girdhar and Alaaeldin El-Nouby. Imagebind: One embedding space to bind them all. In *CVPR*, pages 15180–15190, 2023. 2
- [17] Shuyang Gu and Dong Chen. Vector quantized diffusion model for text-to-image synthesis. In *CVPR*, pages 10696–10706, 2022. 1, 2, 7
- [18] Yuchao Gu and Xintao Wang. Rethinking the objectives of vector-quantized tokenizers for image synthesis. *arXiv preprint arXiv:2212.03185*, 2022. 1
- [19] Yuchao Gu, Xintao Wang, Yixiao Ge, Ying Shan, and Mike Zheng Shou. Rethinking the objectives of vector-quantized tokenizers for image synthesis. In *CVPR*, pages 7631–7640, 2024. 2
- [20] Martin Heusel and Hubert Ramsauer. Gans trained by a two time-scale update rule converge to a local nash equilibrium. *NeurIPS*, 30, 2017. 6
- [21] Frank L Hitchcock. The distribution of a product from several sources to numerous localities. *Journal of mathematics and physics*, 20(1-4):224–230, 1941. 3
- [22] Mengqi Huang and Zhendong Mao. Not all image regions matter: Masked vector quantization for autoregressive image generation. In *CVPR*, pages 2002–2011, 2023. 1, 2
- [23] Mengqi Huang and Zhendong Mao. Towards accurate image coding: Improved autoregressive image generation with dynamic vector quantization. In *CVPR*, pages 22596–22605, 2023. 1, 2
- [24] Minyoung Huh and Brian Cheung. Straightening out the straight-through estimator: Overcoming optimization challenges in vector quantized networks. In *ICML*, pages 14096–14113. PMLR, 2023. 1
- [25] Roy Jonker and Ton Volgenant. A shortest augmenting path algorithm for dense and sparse linear assignment problems. In *DGOR/NSOR: Papers of the 16th Annual Meeting of DGOR in Cooperation with NSOR/Vorträge der 16. Jahrestagung der DGOR zusammen mit der NSOR*, pages 622–622. Springer, 1988. 3
- [26] Diederik P Kingma. Auto-encoding variational bayes. *arXiv preprint arXiv:1312.6114*, 2013. 5
- [27] Doyup Lee and Chiheon Kim. Autoregressive image generation using residual quantization. In *CVPR*, pages 11523–11532, 2022. 2
- [28] Junnan Li, Dongxu Li, Silvio Savarese, and Steven Hoi. Blip-2: Bootstrapping language-image pre-training with frozen image encoders and large language models. In *International conference on machine learning*, pages 19730–19742. PMLR, 2023. 3
- [29] Guotao Liang, Baoquan Zhang, Yaowei Wang, Xutao Li, Yunming Ye, Huaibin Wang, Chuyao Luo, Kola Ye, et al. Lg-vq: Language-guided codebook learning. *arXiv preprint arXiv:2405.14206*, 2024. 1, 2, 5, 6, 7, 8
- [30] Tsung-Yi Lin and Michael Maire. Microsoft coco: Common objects in context. In *ECCV*, pages 740–755. Springer, 2014. 6
- [31] Xinmiao Lin and Yikang Li. Catch missing details: Image reconstruction with frequency augmented variational autoencoder. In *CVPR*, pages 1736–1745, 2023. 1, 2
- [32] Hao Liu and Wilson and Yan. Language quantized autoencoders: Towards unsupervised text-image alignment. *arXiv preprint arXiv:2302.00902*, 2023. 2
- [33] Haotian Liu, Chunyuan Li, Qingyang Wu, and Yong Jae Lee. Visual instruction tuning. *Advances in neural information processing systems*, 36, 2024. 3

- [34] Kechun Liu, Yitong Jiang, Inchang Choi, and Jinwei Gu. Learning image-adaptive codebooks for class-agnostic image restoration. In *CVPR*, pages 5373–5383, 2023. 1
- [35] Ziwei Liu and Ping Luo. Deep learning face attributes in the wild. In *ICCV*, pages 3730–3738, 2015. 6
- [36] Steven Loria et al. textblob documentation. *Release 0.15*, 2(8):269, 2018. 4
- [37] Jiasen Lu and Jianwei Yang. Hierarchical question-image co-attention for visual question answering. *NeurIPS*, 29, 2016. 3
- [38] Yulong Lu and Jianfeng Lu. A universal approximation theorem of deep neural networks for expressing probability distributions. *Advances in neural information processing systems*, 33:3094–3105, 2020. 5
- [39] Ron Mokady and Amir Hertz. Clipcap: Clip prefix for image captioning. *arXiv preprint arXiv:2111.09734*, 2021. 3, 8
- [40] Varun K Nagaraja, Vlad I Morariu, and Larry S Davis. Modeling context between objects for referring expression understanding. In *ECCV*, pages 792–807. Springer, 2016.
- [41] Renjie Pi, Jiahui Gao, Shizhe Diao, Pan, et al. Detgpt: Detect what you need via reasoning. *arXiv preprint arXiv:2305.14167*, 2023. 3
- [42] Stanislav Pidhorskyi, Donald A Adjeroh, and Gianfranco Doretto. Adversarial latent autoencoders. In *CVPR*, pages 14104–14113, 2020. 8
- [43] Alec Radford and Jong Wook Kim. Learning transferable visual models from natural language supervision. In *ICML*, pages 8748–8763. PMLR, 2021. 2
- [44] Alec Radford and Jeffrey Wu. Language models are unsupervised multitask learners. *OpenAI blog*, 1(8):9, 2019. 8
- [45] Colin Raffel and Noam Shazeer. Exploring the limits of transfer learning with a unified text-to-text transformer. *The Journal of Machine Learning Research*, 21(1):5485–5551, 2020. 2
- [46] Mengye Ren and Ryan Kiros. Exploring models and data for image question answering. *NeurIPS*, 28, 2015. 6, 8
- [47] Robin Rombach and Andreas Blattmann. High-resolution image synthesis with latent diffusion models. In *CVPR*, pages 10684–10695, 2022. 1, 7
- [48] Yixuan Su, Tian Lan, Huayang Li, Jialu Xu, Yan Wang, and Deng Cai. Pandagpt: One model to instruction-follow them all. *arXiv preprint arXiv:2305.16355*, 2023. 3
- [49] Yuhta Takida and Takashi Shibuya. Sq-vae: Variational bayes on discrete representation with self-annealed stochastic quantization. *arXiv preprint arXiv:2205.07547*, 2022. 1
- [50] Hugo Touvron, Louis Martin, Kevin Stone, et al. Llama 2: Open foundation and fine-tuned chat models. *arXiv preprint arXiv:2307.09288*, 2023. 2
- [51] Aaron Van Den Oord, Oriol Vinyals, et al. Neural discrete representation learning. *NeurIPS*, 30, 2017. 1, 2, 3
- [52] Cédric Villani. Optimal transport: old and new. 338, 2008. 5
- [53] Catherine Wah and Steve Branson. The caltech-ucsd birds-200-2011 dataset. 2011. 6
- [54] Weihan Wang, Qingsong Lv, Wenmeng Yu, Hong, et al. Cogvlm: Visual expert for pretrained language models. *arXiv preprint arXiv:2311.03079*, 2023. 3
- [55] Zhibiao Wu and Martha Palmer. Verb semantics and lexical selection. *arXiv preprint cmp-lg/9406033*, 1994. 8
- [56] Ling Yang, Jingwei Liu, Shenda Hong, Zhilong Zhang, Zhilin Huang, Zheming Cai, Wentao Zhang, and Bin Cui. Improving diffusion-based image synthesis with context prediction. *Advances in Neural Information Processing Systems*, 36, 2024. 3, 5
- [57] Jiahui Yu and Xin Li. Vector-quantized image modeling with improved vqgan. *arXiv preprint arXiv:2110.04627*, 2021. 2
- [58] Lijun Yu and Yong Cheng. Spae: Semantic pyramid autoencoder for multimodal generation with frozen llms. *arXiv preprint arXiv:2306.17842*, 2023. 2
- [59] Licheng Yu, Patrick Poirson, Shan Yang, Alexander C Berg, and Tamara L Berg. Modeling context in referring expressions. In *ECCV*, pages 69–85. Springer, 2016. 6, 7, 8
- [60] Baoquan Zhang, Huaibin Wang, Chuyao Luo, Xutao Li, Guotao Liang, Yunming Ye, Xiaochen Qi, and Yao He. Codebook transfer with part-of-speech for vector-quantized image modeling. In *CVPR*, pages 7757–7766, 2024. 1, 2, 4, 5, 6, 8
- [61] Chi Zhang, Yujun Cai, Guosheng Lin, and Chunhua Shen. Deepemd: Few-shot image classification with differentiable earth mover’s distance and structured classifiers. In *CVPR*, pages 12203–12213, 2020. 5
- [62] Hang Zhang, Xin Li, and Lidong Bing. Video-llama: An instruction-tuned audio-visual language model for video understanding. *arXiv preprint arXiv:2306.02858*, 2023. 3
- [63] Jiahui Zhang and Fangneng Zhan. Regularized vector quantization for tokenized image synthesis. In *CVPR*, pages 18467–18476, 2023. 1, 6
- [64] Xiaoman Zhang, Chaoyi Wu, Ziheng Zhao, and Lin. Pmcvqa: Visual instruction tuning for medical visual question answering. *arXiv preprint arXiv:2305.10415*, 2023. 3
- [65] Chuanxia Zheng and Andrea Vedaldi. Online clustered codebook. In *ICCV*, pages 22798–22807, 2023. 1, 2, 5, 6, 8
- [66] Yufan Zhou, Ruiyi Zhang, Changyou Chen, Chunyuan Li, et al. Towards language-free training for text-to-image generation. In *CVPR*, pages 17907–17917, 2022. 8
- [67] Yufan Zhou, Bingchen Liu, Yizhe Zhu, Xiao Yang, Changyou Chen, and Jinhui Xu. Shifted diffusion for text-to-image generation. In *CVPR*, pages 10157–10166, 2023. 8
- [68] Deyao Zhu, Jun Chen, Xiaoqian Shen, Xiang Li, and Mohamed Elhoseiny. Minigt-4: Enhancing vision-language understanding with advanced large language models. *arXiv preprint arXiv:2304.10592*, 2023. 2
- [69] Lei Zhu and Fangyun Wei. Beyond text: Frozen large language models in visual signal comprehension. *arXiv preprint arXiv:2403.07874*, 2024. 2